Ferroelectrics Letters Section

ISSN: (Print) (Online) Journal homepage: https://www.tandfonline.com/loi/gfel20

Structural and photoluminescence properties of a trivalent rare earth Sm ion-doped PVA/PVP blend polymer films

C. Salma & B. Hemalatha Rudramadevi

To cite this article: C. Salma & B. Hemalatha Rudramadevi (2022) Structural and photoluminescence properties of a trivalent rare earth Sm ion-doped PVA/PVP blend polymer films, Ferroelectrics Letters Section, 49:1-3, 30-44, DOI: 10.1080/07315171.2022.2076464

To link to this article: https://doi.org/10.1080/07315171.2022.2076464

Published online: 13 Jul 2022.

FERROELECTRICS LETTERS SECTION
2022, VOL. 49, NOS. 1–3, 30–44
https://doi.org/10.1080/07315171.2022.2076464

Structural and photoluminescence properties of a trivalent rare earth Sm ion-doped PVA/PVP blend polymer films

C. Salma and B. Hemalatha Rudramadevi

Department of Physics, Sri Venkateswara University, Tirupati, India

ABSTRACT

Transparent polyvinyl alcohol (PVA)/polyvinylpyrrolidone (PVP) and various concentrations of Sm^{3+} ion-doped PVA/PVP blend-polymer films were prepared using the solution cast method. The structural properties were studied by using XRD and FTIR. Optical UV-Vis, photoluminescence, and decay studies were carried out for prepared PVA/PVP blend polymer films. The XRD confirms the structural change in PVA/PVP blend-polymer with the doping of Sm^{3+} ion. From FTIR, Sm^{3+} ion forms the complex formation within the PVA/PVP polymer structure. The allowed band gap decreased from 5 to 4.6 eV, and the refractive index increased from 2.4 to 2.45, increasing Sm^{3+} ion concentration. From the energy band gap, the bonding parameters (β and δ) were calculated to find the covalent/ionic bond nature of the prepared polymer films. The emission spectra were measured for Sm^{3+}: PVA/PVP with the excitation of 402 nm wavelength ($^6H_{5/2} \rightarrow {}^4F_{7/2}$). $^4G_{5/2} \rightarrow {}^6H_{7/2}$ shows maximum intensity at 0.4 wt % of Sm^{3+}, and beyond concentration, quenching was noticed. It is observed from the decay curve that the lifetime of PVA/PVP samples doped with Sm^{3+} at all concentrations decreases with the increase of Sm^{3+} ion concentration. It was noticed from CIE chromaticity that Sm^{3+}: PVA/PVP blend polymer films are more appropriate for enhancing reddish-orange photonic emission. Based on the above results, Sm^{3+}: PVA/PVP blend polymer films are suitable for reddish-orange luminescent applications.

ARTICLE HISTORY
Received 1 November 2021
Accepted 2 May 2022

KEYWORDS
PVA/PVP blend polymer films; XRD; FT-IR; optical absorption; photoluminescence

1. Introduction

In recent years, researchers have noticed that polymer film synthesis doped with transition metal ions and rare-earth ions forms the novel multifunctional compounds for an extensive area of applications [1]. A Blend type polymer or polymer mixture type of compound is a member of such a class of materials. Not less than two polymers can be blended mutually to form an innovative compound material with novel properties. Moreover, polymer blending is an inexpensive procedure to fabricate polymer materials with modified structural and physical properties, which do not exist in a single polymer [2]. Because of these enhanced and novel properties find potential applications are used in photonic devices, polymer solar cells, nonlinear optics, and optical switching [3].

CONTACT B. Hemalatha Rudramadevi drbhrd@gmail.com
Communicated by Dr George W Taylor

Polyvinyl alcohol (PVA) and polyvinyl pyrrolidone (PVP) have significant priority depending on doping with various materials owing to their ability of film developing with fine optical quality, semi-crystalline nature, controllable optical and electrical characteristics [3]. PVA is used in the formation due to its distinctive physical and chemical properties like a possibility with diverse molecular weights, non-toxicity, solubility in water [4]. "The formation of supermolecules in PVA is vital because it functions as a functional material" [5]. The supermolecular model and structure depend on non-covalent forces like hydrogen and coordinate bonds [6]. Polyvinyl pyrrolidone (PVP) is a low-priced polymer eminently soluble in water and alcohol. PVP has a higher glass transition temperature (T_g) because of the occurrence of the pyrrolidone group (C = O) in the side chains of PVP, which forms composite formation [7]. When the PVA is blended with PVP, the interactions occur among the OH group of PVA and a proton-accepting carbonyl group of PVP [8], owing to a wide diversity of applications at the present generation science and technology. The Lanthanide ions can form complex polymer materials for three principal reasons, namely (1) Relatively large ionic size, (2) Tendency to develop a covalent bond, and (3) Low electrostatic interaction together with the polar groups of the polymer material [9].

Rare earth elements (REEs) show a significant impact on the structure of polymers, particularly PVA and PVP. The REE complexes in their trivalent state contain strongly electronegative donor atoms. Potential oxygen donors are also present in the PVA and PVP. In this way, it interacts with rare-earth ions and forms PVA/PVP- rare earth complexes. Rare-earth ion doped polymer blends are used as light converting molecular devices (LCMDS); it opens a new class of flexible resources for photonic applications [10]. Among the rare-earth ions, samarium (Sm^{3+}) emits the reddish-orange emission attributed to the electronic transition of $^4G_{5/2} \rightarrow {}^6H_{7/2}$ under ultraviolet (UV) excitation at 400 nm, and it shows high luminescent efficiency. Rare-earth ions, light emission, depending on the chemical environment [11]. Samarium doped polymer composites, glasses, and ceramics illustrate prominent reddish-orange emission and display devices.

The present work intention was to prepare host PVA/PVP blend polymer and samarium doped PVA/PVP blend polymer films to look at their function on changes of its structural, optical, and photoluminescence properties.

2. Experimental studies

2.1. Sample preparation

The study of blended polymer films was prepared using the solution cast method. Polyvinyl alcohol (PVA) [M. W = 1,25,000], Polyvinyl pyrrolidone (PVP) [M. W = 13,00,000] and samarium nitrate hexahydrate [Sm (NO_3). $6H_2O$] was used with a purity of 99.9%. The weight percent required quantity of samarium nitrate (0.0, 0.1, 0.2, 0.3, 0.4, and 0.5 weight%) was dissolved in 30 ml of doubly distilled water under continuous stirring until the viscous solution was formed. The viscous solution was left for one day to get a non-bubbled solution. Then the polymeric solution was cast onto cleaned polypropylene dishes and desiccated at room temperature for four days. After exhaust, the polymer films were peeled off the Petri dishes and placed in the vacuum desiccators. The prepared polymer film thickness was 0.01 cm.

2.2. Characterization

X-ray diffraction study was carried out for the pure PVA/PVP, and Sm^{3+} doped blend polymer film using Shimadzu model XRD-6000 diffractometer with monochromatic Cuk_{α} radiation of wavelength $\lambda = 1.5418$ Å and Bragg's the angle 2θ in the range of 10° to 60°. Jasco FT-IR 430 spectrometer was used to record the prepared polymer films, functional groups of PVA/PVP, and Sm^{3+}: PVA/PVP with a wavenumber range from 800 to 4000 cm^{-1}. The optical parameters for PVA/PVP and Sm^{3+}: PVA/PVP blend polymer films were measured in the UV-Vis-NIR region using Perkin Elmer Lambda 950. Emission spectra and lifetime were obtained using Edinburg UV-Vis-NIR FLS-980 Fluorimeter with Xenon flash lamp.

3. Results and discussion

3.1. X-Ray diffraction

X-ray diffraction (XRD) spectra for host PVA/PVP blended polymer film and Sm^{3+} doped polymer films in the range between 10° and 60° were recorded and presented in Figure 1. From the XRD, two diffraction peaks were noticed around 2θ, equaled15°, and 22°. A strong diffraction peak at 22° corresponds to the following reflection plane (2 0 0), which was assigned to previous literature work (JCPDS card No. 65-2870) [12, 13]. The two peaks were related to the semi-crystalline nature of pure PVA/PVP and Sm^{3+}: PVA/PVP blend polymer films. With the increase of Sm^{3+} ion concentration in PVA/PVP film, the peak profile gradually decreases its intensity. It is observed that the peak intensity at $2\theta = 15°$ and 22° decreases, and the width of these peaks increase

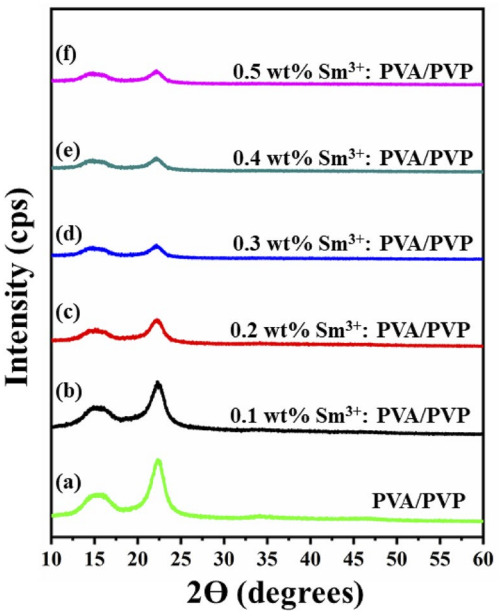

Figure 1. XRD pattern of (a) pure PVA/PVP (b-f) 0.1 to 0.5 wt% Sm^{3+}: PVA/PVP blend polymer films.

Table 1. XRD crystalline parameters for the pure and Sm^{3+}: PVA/PVP blend polymer films.

(wt%) Sm^{3+}: PVA/PVP	Crystallite size (D) (nm)	Dislocation density (δ) $(nm)^{-2}$	Crystallite separation (R) Å
0.0	5.90	0.028	5.06
0.1	5.61	0.031	5.04
0.2	5.43	0.033	5.02
0.3	4.97	0.040	5.01
0.4	4.51	0.049	4.98
0.5	4.49	0.050	4.96

with increasing Sm^{3+} ion from 0.1 to 0.5 weight% as shown in Figure 1 and noticed that the decrease in crystalline size. This is because interactions between the PVA/PVP blend polymer and the Sm^{3+} ions lead to the decline in the intermolecular interaction amongst the PVA/PVP polymer chains and the degree of crystalline [14]. New diffraction peaks were not noted with the Sm^{3+}: PVA/PVP polymer film, signifying through dissociation of the Sm^{3+} ion into the PVA/PVP blend polymer film. From the XRD graph, various crystalline parameters were calculated using the below formulae and presented in Table 1 for the pure and Sm^{3+}: PVA/PVP blend polymer films for the peak at 22°, the maximum in peak intensity.

The particle size can be calculated by the Debye–Scherrer's formula [15, 16]

$$D = \frac{k\lambda}{\beta \cos\theta} \tag{1}$$

Where β is the full width at the half maxima (in radians), k is a constant (~0.9), λ is the wavelength (0.154 nm), θ is the angle of diffraction, and D is the particle size in nm.

$$\text{Dislocation density } \delta = \frac{1}{D^2} \tag{2}$$

$$\text{Average separation between the crystallites } R = \frac{5\lambda}{\beta \sin\theta} \tag{3}$$

From Table 1, it is noticed that pure crystalline parameters were initiated to be 5.90 nm, 0.028 nm^{-2}, and 5.06 Å related to crystalline size, dislocation density, and crystalline separation, respectively. Crystalline size and separation parameters decreased with an increase in samarium concentration. These magnitudes range between 5.61 and 4.49 nm, 0.031 and 0.050 nm^{-2}, and 5.04 and 4.96 Å ascribed to D, δ, and R, respectively.

3.2. FTIR studies

The FTIR spectra of pure and Sm^{3+}: PVA/PVP blend polymers were examined in the range from 4000 to 800 cm^{-1} and shown in Figure 2. In the pure PVA/PVP and Sm^{3+}: PVA/PVP FTIR spectra, at 1057 cm^{-1}, a weak band was ascribed to OH bending [17].

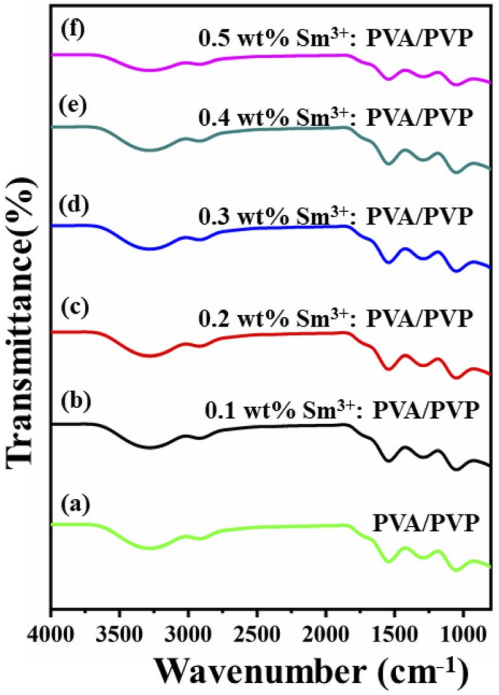

Figure 2. FT-IR spectra of (a) pure PVA/PVP (b-f) 0.1 to 0.5 wt% Sm^{3+}: PVA/PVP blend polymer films.

Bands observed at 1273 cm^{-1}, and 1541 cm^{-1} correspond to an acetyl group of C-O stretching vibration and C = N (Pyridine ring) band, respectively [18]. Asymmetric stretching of the CH_2 methylene group appears at 2910 cm^{-1} [14]. The strong and broadband noticed at 3267 cm^{-1} is associated with the OH hydroxyl groups stretching mode, a unique characteristic band of alcohols [19]. The 3267 cm^{-1} band shifted to 3257 cm^{-1} for Sm^{3+}: PVA/PVP; this nature of shifting the band toward lower frequency is ascribed to stronger hydrogen bonding [4]. With the addition of Sm^{3+} at different concentrations to PVA/PVP blend polymer, asymmetrical shifts are observed.

The shifted bands indicate the magnification of crystalline reduction caused by the interactions among the adjacent OH groups of PVA and Sm^{3+} via Intra/intermolecular hydrogen bonding and, therefore, the decrease in the crystalline order. This is owing to the strong bonding of ion-ligand complexes [20]. The XRD data confirmed this hypothesis. The non-uniform shifts ascribed in the Sm^{3+} doped PVA/PVP spectra are mainly because hydroxyl groups present in the PVA chain initiate stable and complex compounds or because of bonding with these substances [4]. The increase in the addition of Sm^{3+} ion concentration results in a slight shift in the band positions. The dissimilarity in the bands intensity upon doping of Sm^{3+} leads to more vital interaction among the PVA/PVP polymer blend and Sm^{3+} [18].

3.3. Optical absorption studies

Figure 3 represents the absorption spectrum of pure blend polymer in 200 nm to 1000 nm. The pure PVA/PVP polymer film spectrum has a small band at 222 nm,

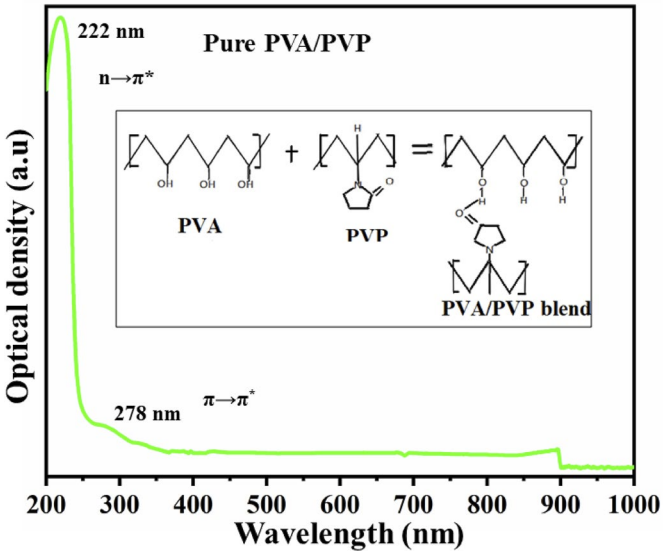

Figure 3. Absorption spectra of pure PVA/PVP blend polymer film.

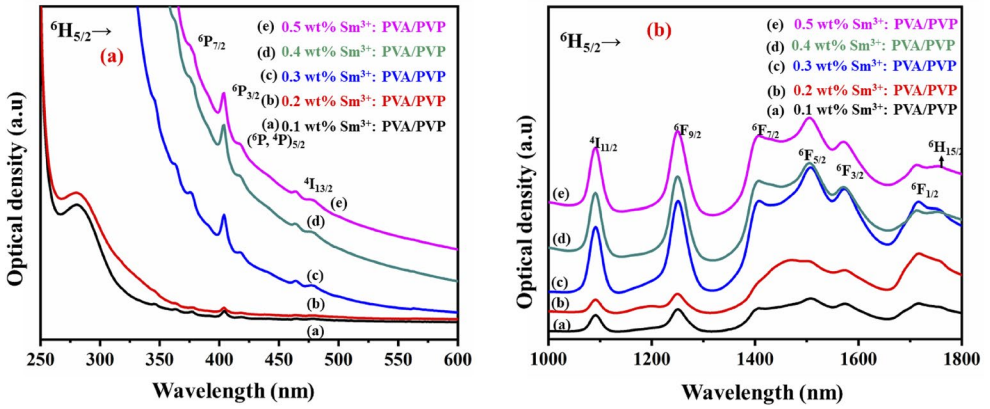

Figure 4. Optical absorption spectra of 0.1 to 0.5 wt% Sm^{3+}: PVA/PVP blend polymer films in (a) Uv-Visible and (b) NIR region.

which attributes to n→π* transition representing the semi-crystalline nature of PVA/PVP polymer film [21, 22]. One other band was noticed a shoulder at 278 nm owing to π→π* transition, which comes from unsaturated bonds, primarily (C = O and/or C = C) [18], FTIR verified the results. From Figure 4(a), a redshift is noticed in absorption bandwidth increase the Sm^{3+} ion concentration in PVA/PVP blend polymer. This shift indicates the complication between the Sm^{3+} ions in PVA/PVP blend polymer film and may also be in effect of change in crystalline due to the addition of Sm^{3+} ions [18]. Sm^{3+}: PVA/PVP polymer film absorption spectra observed in UV-Visible and near-infrared regions (NIR) regions are presented in Figure 4(a,b) correspondingly. Sm^{3+}: PVA/PVP polymer film absorption spectra have exhibits eleven absorption bands in UV-Visible and NIR region and were belongs to $^6H_{5/2} \rightarrow {}^6P_{7/2}$, $^6P_{3/2}$, $(^6P, {}^4P)_{5/2}$, $^4I_{13/2}$,

Table 2. Absorption peak positions and energies along with their assignments of Sm^{3+}: PVA/PVP blend polymer films.

Transition from $^6H_{5/2}$	Peak position λ (nm)	Energy (cm^{-1}) Crystal Aqua (υ_c) (υ_a)		$\beta = \upsilon_c/\upsilon_a$
$^6P_{7/2}$	377	26525	26660	9.9
$^6P_{3/2}$	403	24630	24999	0.98
$(^6P, ^4P)_{5/2}$	417	23980	24101	0.99
$^4I_{13/2}$	464	21551	21650	0.99
$^4I_{11/2}$	479	20876	21096	0.98
$^6F_{9/2}$	1092	91575	9136	10.02
$^6F_{7/2}$	1250	80000	7977	10.02
$^6F_{5/2}$	1403	71275	7131	9.99
$^6F_{3/2}$	1504	66489	6641	10.01
$^6F_{1/2}$	1569	63734	6397	9.96
$^6H_{15/2}$	1713	58377	46	1269.06

$\bar{\beta}$ = 121.18, δ = −0.99

$^4I_{11/2}$,$^6F_{9/2}$,$^6F_{7/2}$, $^6F_{5/2}$, $^6F_{3/2}$, $^6F_{1/2}$ and $^6H_{15/2}$ transitions with the wavelength 377, 403, 417, 464, 479, 1092, 1250, 1403, 1504, 1569 and 1713 nm respectively [23]. Most of the observed transitions in the UV-NIR spectra were originated because of the induced electric dipole interactions as per the selection rule $\Delta J \leq 6$. The intense band existed in the NIR region due to the 4f electrons, which are successfully shielded with the filled 5 s and 5p shells $^6H_{5/2} \rightarrow {}^6F_{1/2}$ and $^6H_{5/2} \rightarrow {}^6F_{3/2}$ are the hypersensitive transitions for the Sm^{3+} ion, and that satisfies the selection rules $|\Delta S| = 0$, $|\Delta J| \leq 2$ and $|\Delta L| \leq 2$ [24]. The position, shape and intensity of the electronic transitions were sensitive to the ligand field. In the NIR region, the transitions are spin allowed at $\Delta S = 0$ and therefore shows high-level sensitivity. The nephelauxetic ratio (β) and bonding parameters were obtained from the absorption energy bands and discriminated the nature of Sm^{3+} ion ligand bond in the present work and presented in Table 2. The nephelauxetic ratio (β) is evaluated with the succeeding relation [25]:

$$\beta = \frac{\upsilon_c}{\upsilon_a} \tag{4}$$

$$\bar{\beta} = \frac{\sum \beta}{N} \tag{5}$$

Where υ_c is the electronic transition wave number of crystals in cm^{-1} and υ_a is the wavenumber (cm^{-1}) for the same transitions of the aqua solution of Sm^{3+} ion. From the average values of $\bar{\beta}$ the bonding factor δ was calculated with the following relation [25]:

$$\delta = \frac{1 - \bar{\beta}}{\bar{\beta}} \tag{6}$$

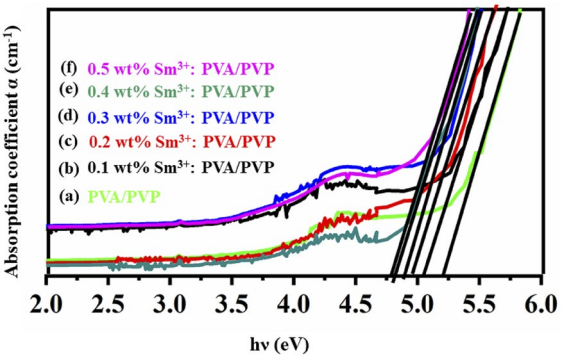

Figure 5. The absorption coefficient α versus photon energy hυ of (a) pure PVA/PVP (b–f) 0.1 to 0.5 wt% Sm^{3+}: PVA/PVP films.

Table 3. Absorption edge, indirect bandgap, and refractive index for pure PVA/PVP and Sm^{3+}: PVA/PVP blend polymer films.

Sample	Absorption edge (eV)	Indirect bandgap energy (eV)	Refractive index (n)
PVA/PVP	5.2	5	2.40
0.1 wt% Sm^{3+}: PVA/PVP	5.05	4.9	2.41
0.2 wt% Sm^{3+}: PVA/PVP	4.9	4.8	2.42
0.3 wt% Sm^{3+}: PVA/PVP	4.84	4.75	2.43
0.4 wt% Sm^{3+}: PVA/PVP	4.82	4.69	2.4
0.5 wt% Sm^{3+}: PVA/PVP	4.7	4.6	2.45

The bonding parameter can be positive or negative depending on the ambient environment field, illustrating covalent or ionic bonding. In this work, the negative values (−0.99) accomplished for the bonding parameter shows the ionic nature of the Sm^{3+} ion.

3.3.1. Optical energy gap

For a better analysis of the optical properties of the prepared blended polymer films, the absorption coefficient (α) was helpful, and it was calculated from the relation [5] and shown in Figure 5.

$$\alpha = 2.303^{\star}\frac{A}{t} \tag{7}$$

where A is the absorbance of the film and t is the thickness of the blended polymer film. The absorption edge values obtained from the Tauc plots of α versus hυ and presented in Table 3. It is noticed that the absorption coefficient was increased with the increment in the concentration of Sm^{3+} ions. The analysis of the primary absorption edge contributes the most helpful information regarding the absorption band structure and the optical bandgap of the blended polymer material [26–28]. Owing to the expression of Tauc, Davis, and Mott [29] described in the vicinity of the fundamental band-edge for the allowed indirect transitions is occurring, and this can be observed by plotting a graph between $(\alpha h\upsilon)^{1/2}$ v_s photon energy [30].

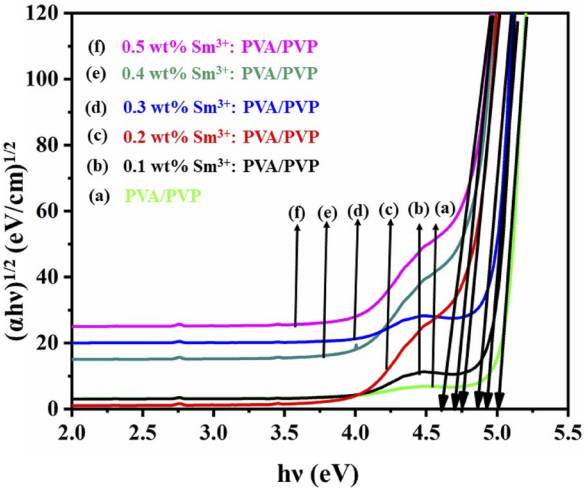

Figure 6. Tauc Plots of $(\alpha h\upsilon)^{1/2}$ with $(h\upsilon)$ for (a) pure PVA/PVP (b–f) 0.1 to 0.5 wt% Sm^{3+}: PVA/PVP blend.

$$(m\alpha h\upsilon)^{1/2} = C(h\upsilon - Egi) \tag{8}$$

where $h\upsilon$ is the photon energy, E_{gi} is the indirect bandgap energy, m is the integer, C is constant. From Figure 6, Indirect bandgap values deliberated from the extrapolating $(\alpha h\upsilon)^{1/2}$ =0 for the indirect transitions and values were listed in Table 3. The optical energy gap value reduces with the Sm^{3+} ion concentration increases in PVA/PVP blend polymer. Sm^{3+} ion concentration is the main cause for the formation of defects in the blend polymer films. The defects create the localized states in the PVA/PVP optical bandgap. The inflation may also interpret the reduction in the energy bandgap in the degree of disorder in prepared samples, which occurs because of the change in polymer structure [5]. Specifically, the decreases in bandgap energy consider the optimization in the degree of disarrangement in the films. The XRD well supports the results mentioned above. Decreasing the optical bandgap of blend polymer materials is considered for interesting applications and designing different potential optical devices [31, 32].

3.3.2. Refractive index

The refractive index is crucial in optical communication systems and designing devices based on spectral dispersion [33]. Therefore, the following equation calculated the refractive index (n) for the prepared samples using the bandgap values [34].

$$n = \sqrt{\frac{12.417}{\sqrt{Eg - 0.365}}} \tag{9}$$

Table 3 represents the refractive index values for PVA/PVP and Sm^{3+}: PVA/PVP blend polymer films. From Table 3, minor variations are observed in the refractive

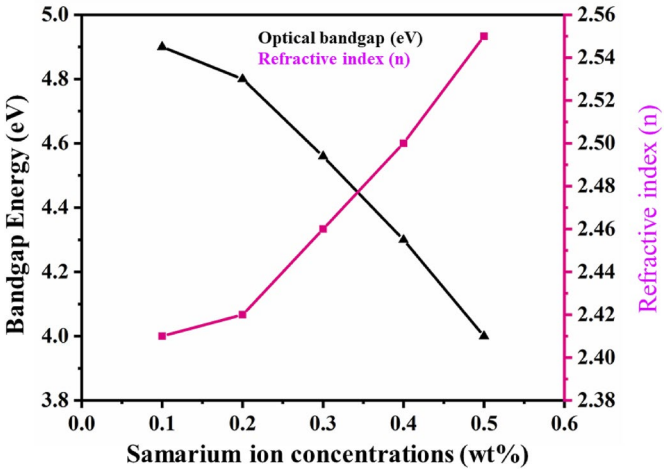

Figure 7. Plots of optical bandgap and refractive index of 0.1 to 0.5 wt% Sm^{3+}: PVA/PVP blend polymer films.

index values for PVA/PVP blend polymer and Sm^{3+}: PVA/PVP, even though a strong effect is noticed in the refractive index of Sm^{3+}: PVA/PVP correlates with PVA/PVP blend polymer film. From Figure 7, the refractive index increases with Sm^{3+} ion concentration in PVA/PVP. The highest refractive index value (2.55) was obtained for the 0.5 wt% Sm^{3+}: PVA/PVP. The maximum refractive index is a sign of high density of PVA/PVP: Sm^{3+} ions owing to the integration of Sm^{3+} ions present in the primary chain of the PVA/PVP polymer blend. The thickness of the blended polymer film and the dependency of the refractive index on the film density can be examined by the Clausius-Mossotti equation [35]. At present, the high refractive index of rare-earth-doped polymers is widely used in potential applications along with display devices, optical communication, anti-reflective coatings, and various semiconductors reported by Ali et al. [3]. A strong interrelationship is noticed among the bandgap energy and refractive index, increasing Sm^{3+} ion concentration. The bandgap decreased and refractive index increased was observed, and they are inversely related to each other. In addition to this, a big difference between optical bandgap and refractive index values of Sm^{3+}: PVA/PVP was observed. This result indicates the intensive and robust effect of Sm^{3+} ions on the optical parameters of the PVA/PVP blended polymer. Figure 7 represents the variation in the optical bandgap and refractive index values of PVA/PVP and Sm^{3+}: PVA/PVP blend polymer film.

3.4. Photoluminescence properties

The excitation spectra of Sm^{3+}: PVA/PVP blend polymer film recorded with known emission wavelength 596 nm for these polymer films are shown in Figure 8(a). Four peaks were noticed from the excitation spectra to signify the electronic transitions of samarium ion, i.e. $^6H_{5/2} \rightarrow {}^4H_{9/2}$ (346 nm), $^6H_{5/2} \rightarrow {}^4D_{1/2}+ {}^6P_{7/2}$ (376 nm), $^6H_{5/2} \rightarrow {}^4F_{7/2}$ (403 nm), and $^6H_{5/2} \rightarrow {}^4G_{9/2}$ (440 nm). Among these, the prominent excitation peak is 403 nm ($^6H_{5/2} \rightarrow {}^4F_{7/2}$). Of all the excitation peaks, the peak at 403 nm attributed to the transition $^6H_{5/2} \rightarrow {}^4F_{7/2,}$ employed as excitation wavelength to measure the emission

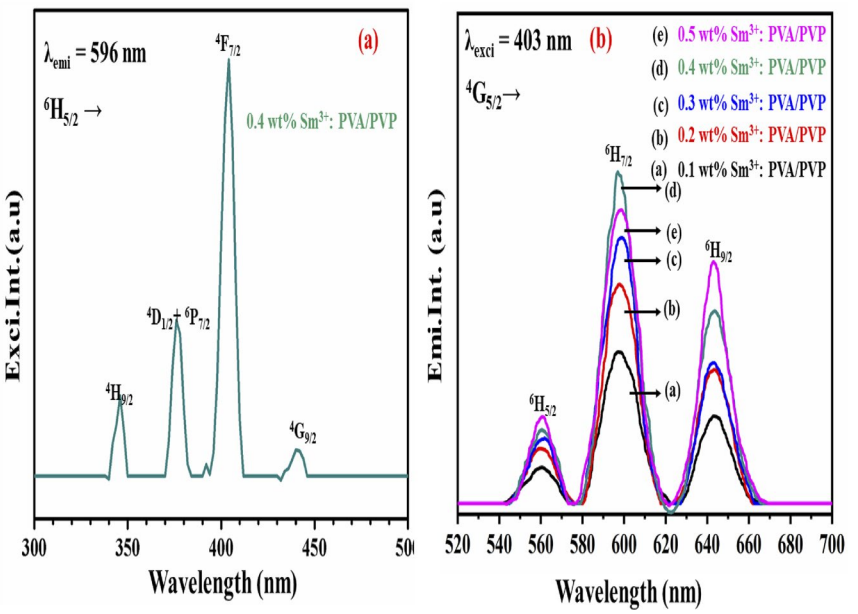

Figure 8. Photoluminescence spectra: (a) 0.4 wt% Sm^{3+}: PVA/PVP excitation spectra (b) Emission spectra of 0.1 to 0.5 wt% Sm^{3+}: PVA/PVP blend polymer films.

spectra. Figure 8(b) demonstrates the emission spectra of Sm^{3+}: PVA/PVP blend polymer films in the spectral range 500–700 nm while maintaining the excitation wavelength at 403 nm. The spectra have three emission peaks at about 560 nm, 596 nm, and 643 nm corresponding to the electronic transitions of $^4G_{5/2} \rightarrow {}^6H_{5/2}$, $^4G_{5/2} \rightarrow {}^6H_{7/2,}$ and $^4G_{5/2} \rightarrow {}^6H_{9/2,}$ respectively. Among these electronic transitions, $^4G_{5/2} \rightarrow {}^6H_{7/2}$ (596 nm) [reddish orange] has an extreme radiative intensity compared to other electronic transitions $^4G_{5/2} \rightarrow {}^6H_{5/2}$ (560 nm), and $^4G_{5/2} \rightarrow {}^6H_{9/2}$ (643 nm) is in the visible range [36]. Thus, the electronic transition $^4G_{5/2} \rightarrow {}^6H_{7/2}$ is helpful for laser emission. By the selection rules [3], $\Delta J = 0, \pm 1$ for a magnetic dipole (MD) transitions and electric dipole (ED) transitions yield to $\Delta J \leq 6$ expect J or $J^1 = 0$ when $\Delta J = 2$, 4 and 6. Therefore, the electronic transitions $^4G_{5/2} \rightarrow {}^6H_{5/2}$ ($\Delta J = 0$) at 560 nm, $^4G_{5/2} \rightarrow {}^6H_{7/2}$ ($\Delta J = 1$) at 596 nm are MD transitions, and $^4G_{5/2} \rightarrow {}^6H_{9/2}$ ($\Delta J = 2$) at 643 nm is ED transition. From the emission spectra, it is noticed that with an increase in concentration from 0. 1 to 0.4 wt%, the emission intensity increases, and the highest output emission intensity is noticed for the 0.4 weight% of Sm^{3+}: PVA/PVP above that concentration quenching was observed and was shown in Figure 8(b). This concentration quenching was noticed at 0.5 wt % of Sm^{3+} ion concentration because of resonance energy transfer among the excited Sm^{3+} ions at greater concentrations. Sm^{3+}: PVA/PVP blend polymer films equivalent energy level diagram and their emission transitions are shown in Figure 9.

3.4.1. Decay analysis

The decay profile for the $^4G_{5/2}$ state of Sm^{3+}: PVA/PVP polymer samples was measured under an excitation of 400 nm wavelength and emission at 596 nm, presented in Figure 10. From the figure, it was noticed that the decay curves of the $^4G_{5/2}$ level had

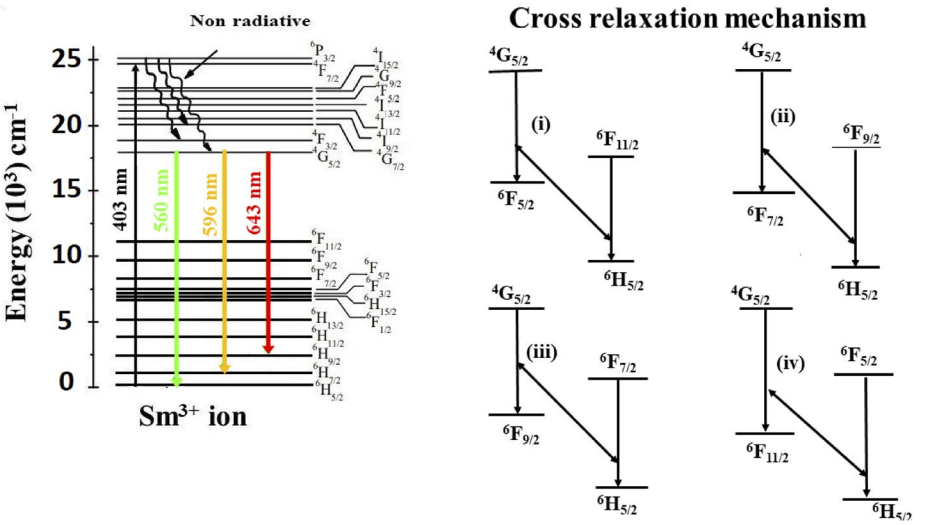

Figure 9. Energy level diagram showing emission mechanism and cross-relaxation Mechanism in Sm^{3+}: PVA/PVP blend polymer films.

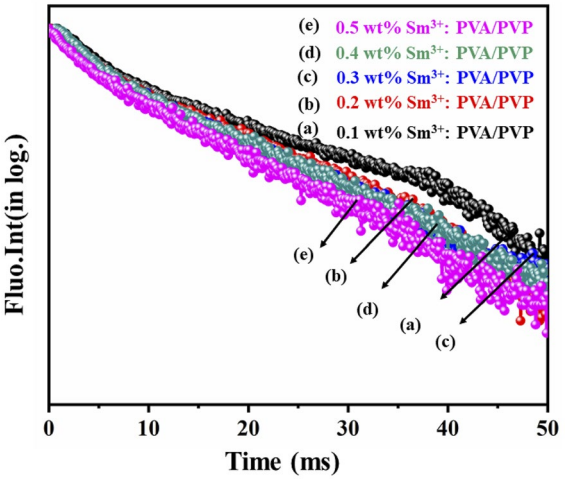

Figure 10. Decay profile of 0.1 to 0.5 wt% of the Sm^{3+}: PVA/PVP blend polymer films.

demonstrated a non-exponential nature because of the existence of non-radiative energy transfer. Therefore, the decay time has been evaluated, and the values are 9.9 ms for 0.1 wt %, 8.8 ms for 0.2 wt %, 8.7 ms for 0.3 wt %, 8.1 ms for 0.4 wt %, and 7.7 ms for 0.5 wt % of Sm^{3+}: PVA/PVP polymers. In addition, it was noticed that the lifetime values were decreased with an increase in Sm^{3+} ion concentrations because of energy transfer beyond cross-relaxation and resonant energy transfer among Samarium ions.

3.4.2. Chromaticity color coordinates

The CIE chromaticity diagram (Commission Internationale del'Eclairage) color coordinates were evaluated from the emission spectra with CIE 1931 chromaticity for the

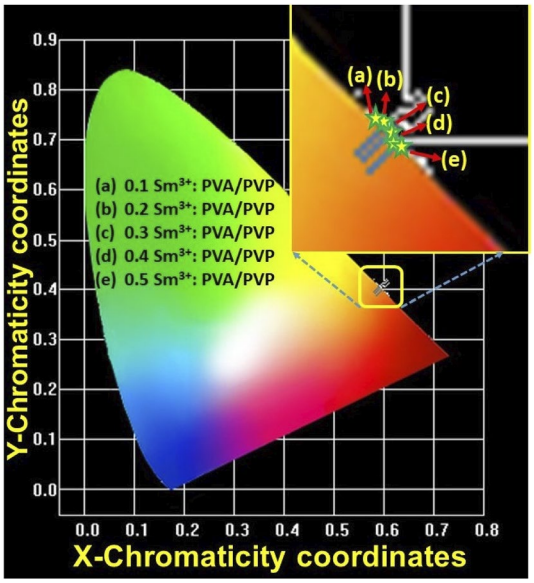

Figure 11. CIE chromaticity diagram of the (a–e) 0.1 to 0.5 wt% Sm^{3+}: PVA/PVP blend polymer films.

Table 4. CIE coordinates and CCT values of Sm^{3+} ions in PVA/PVP blend polymer films at λ_{emi} = 596 nm wavelength.

Name of the sample	CIE color coordinates (x, y)	CCT
0.1 wt% Sm^{3+}: PVA/PVP	(0.5949, 0.4044)	1507
0.2 wt% Sm^{3+}: PVA/PVP	(0.5920, 0.4072)	1535
0.3 wt% Sm^{3+}: PVA/PVP	(0.5978, 0.4014)	1477
0.4 wt% Sm^{3+}: PVA/PVP	(0.5969, 0.4023)	1486
0.5 wt% Sm^{3+}: PVA/PVP	(0.5981, 0.4011)	1474

entire concentrations of Sm^{3+} ion in PVA/PVP polymer and shown in Figure 11. The CIE color coordinates (x, y) and correlated color temperature (CCT) values were calculated for the Sm^{3+}: PVA/PVP blend polymer films and are given in Table 4. "CCT values signify the emergence of light as cool or warm. Usually, it is well-known that the lamps with CCT < 3200 K emit warm light while those with CCT > 4000 K were given cool white light" [36]. This work observed CCT values for the Sm^{3+}: PVA/PVP polymer samples more than 4000 K, which is helpful for warm white light. It was noticed that the CIE values are positioned in the reddish-orange region equivalent to $^4G_{5/2} \rightarrow {}^6H_{7/2}$ (596 nm) electronic transition. So, the prepared Sm^{3+}: PVA/PVP blend polymer films are relevant for promoting reddish-orange lighting devices.

4. Conclusions

The present work studied the structural and optical properties of Sm^{3+}: PVA/PVP blend polymer films. XRD studies revealed a decline in the degree of crystallinity and crystalline size owing to Sm^{3+} ions merger in the PVA/PVP blend polymer. FTIR analysis affirms the complex nature and interconnecting bond formation among the PVA/PVP polymer and Sm^{3+} ion. Reducing the indirect bandgap of pure PVA/PVP

from 5.2 eV to 4.7 eV illustrates interactions among the PVA/PVP and Sm^{3+} ion. The refractive index enhances with the increase of Sm^{3+} ion concentrations. The configuration of intermolecular interaction and complication involving PVA/PVP and Sm^{3+} was verified by using XRD, FTIR, and optical absorption studies. From the emission spectra, Sm^{3+}: PVA/PVP blend polymer films show a significant emission peak at 596 nm (reddish-orange) with an excitation of 400 nm. Concentration quenching was observed at 0.5 wt% of Sm^{3+}: PVA/PVP polymers, which indicated that 0.4 wt % of Sm^{3+} ion be the optimum concentration. Reddish-orange emission (0.5969, 0.4023 of 0.4 wt%) possessed by these blend polymer films is also proved by CIE chromaticity. From all these studies, it was concluded that Sm^{3+}: PVA/PVP blend polymer films were helpful in the development of optical devices.

References

1. F. M. Ali, I. M. Ashraf, and S. M. Alqahtani, Promising Cu-doped polyvinyl alcohol films for optical and photoconductive applications, *Physica B.* **527**, 24 (2017). DOI: 10.1016/j.physb.2017.09.107.
2. B. S. Hariharan *et al.*, Studies on NiO-PVA composite films for optoelectronics and optical limiters, *IEEE Photon. Technol. Lett.* **30** (17), 1539 (2018). DOI: 10.1109/LPT.2018.2859042.
3. S. Choudhary, Characterization of amorphous silica nanofiller effect on the structural, morphological, optical, thermal, dielectric, and electrical properties of PVA-PVP blend based polymer nanocomposites for their flexible nanodielectric applications, *J. Mater. Sci: Mater. Electron.* **29** (12), 10517 (2018). DOI: 10.1007/s10854-018-9116-y.
4. A. Hashim, I. R. Agool, and K. J. Kadhim, Novel of (polymer blend-Fe_3O_4) magnetic nanocomposites: preparation and characterization for thermal energy storage and release, gamma ray shielding, antibacterial activity and humidity sensors applications, *J. Matter.Sci.: Matter. Electron.* **29**, 10369 (2018).
5. M. Abdelaziz, Cerium doping effects on optical and thermal properties of PVA films, *Physica B.* **406** (6–7), 1300 (2011). DOI: 10.1016/j.physb.2011.01.021.
6. K. P. Mortl *et al.*, Structure and magnetic characteristics of an oxalate-bridged U(IV)-Mn(II) three dimensional network, *Inorg. Chem.* **39**, 1626 (2000).
7. M. Ravi *et al.*, Investigations on electrical properties of PVP: KIO4 polymer electrolyte films, *Solid State Sci.* **19**, 85 (2013). DOI: 10.1016/j.solidstatesciences.2013.02.006.
8. M. Premalatha *et al.*, Characterization blend polymer PVA-PVP complexed with ammonium thiocyanate, *Ionics* **22** (8), 1299 (2016). DOI: 10.1007/s11581-016-1672-7.
9. A. Fernandes *et al.*, Study of new lanthanide complexes of 2,6-pyridinedicarboxylate: Synthesis, Crystala structure of Ln(Hdipic) (dipic) with Ln = Eu, Gd, Tb, Dy, Ho, Er, Yb, luminescence properties of Eu (Hdipic) (dipic), *Polyhedron* **20** (18), 2385 (2001). DOI: 10.1016/S0277-5387(01)00841-5.
10. Y. Han *et al.*, Controlled synthesis and luminescence properties of doped NaLa(WO4)2 microstructures, *J. Ind. Eng. Chem.* **34**, 269 (2016). DOI: 10.1016/j.jiec.2015.11.021.
11. K. N. Kumar *et al.*, Dazzling red emission from TiO_2 nanoparticles impregnated co-doped Gd^{3+}+Eu^{3+}: PVA polymer nanocomposites for photonic applications, *J. Ind. Eng. Chem.* **45**, 349 (2017). DOI: 10.1016/j.jiec.2016.10.002.
12. A. M. Mostafa, and A. A. Menazea, Polyvinyl alcohol/silver nanoparticles film prepared via pulsed laser ablation: An eco-friendly nano-catalyst for 4-nitrophenol degradation, *J. Mol. Struct.* **1212**, 128125 (2020). DOI: 10.1016/j.molstruc.2020.128125.
13. M. J. Tommalieh, N. S. Awwad *et al.*, Characterization and electrical enhancement of PVP/PVA matrix doped by gold nanoparticles prepared by laser ablation, *Radiat. Phys. Chem.* **179**, 109195 (2021). DOI: 10.1016/j.radphyschem.2020.109195.

14. E. M. Abdelrazek, I. S. Elashmawi, and S. Labeeb, Chitosan filler effects on the experimental characterization, spectroscopic investigation and thermal studies of PVA/PVP blend films, *Physica B.* **405** (8), 2021 (2010). DOI: 10.1016/j.physb.2010.01.095.
15. Basavarajeshwari, M. Baraker, and B. Lobo, Experimental studies of PVA-PVP blend films doped with cadmium chloride monohydrate, *Indian J. Pure Appl. Phys.* **54**, 634 (2016).
16. R. J. Sengwa, and S. Choudhary, Structural characterization of hydrophilic polymer blends/montmorillonite clay nanocomposites, *J.Appl. Polym. Sci.* **131**, 40617 (2014).
17. M. Abdelaziz, and E. M. Abdelrazek, Effect of dopant mixture on structural, optical and electron spin resonance properties of polyvinyl alcohol, *Physica B.* **390** (1–2), 1 (2007). DOI: 10.1016/j.physb.2006.07.067.
18. E. M. Abdelrazek *et al.*, Structural, optical, thermal and electrical studies on PVA/PVP blends filled with lithium bromide, *Curr. Appl. Phys.* **10** (2), 607 (2010). DOI: 10.1016/j.cap.2009.08.005.
19. T. A. Hamdalla, and T. A. Hanafy, Optical properties studies for PVA/Gd, La, Er or Ychlorides based on structural modification, *Optik* **127** (2), 878 (2016). DOI: 10.1016/j.ijleo.2015.10.187.
20. H. Elhosiny Ali, Y. Khairy *et al.*, Optical spectroscopy and electrical analysis of La^{3+}-doped PVA composite films for varistor and optoelectronic applications, *J. Mater. Sci: Mater. Electron.* **29** (23), 20424 (2018)., DOI: 10.1007/s10854-018-0176-9.
21. [21N. B. Rithin Kumar *et al.*, Microstructural and mechanical studies of PVA doped with Zno and WO_3 composites films, *J. Polym.* **2014**, 1 (2014). DOI: 10.1155/2014/846140.
22. R. F. Bhajantri *et al.*, Studies on fluorescent PVA + PVP + MPDMAPP composite films, *Polym. Eng. Sci.* **49** (5), 903 (2009). DOI: 10.1002/pen.21341.
23. G. Seeta Rama Raju, and S. Buddhudu, Photoluminescence analysis of Sm^{3+} and Dy^{3+}doped PVA films, *J. Appl. Polym. Sci.* **107** (4), 2480 (2008). DOI: 10.1002/app.27257.
24. C. Madhukar Reddy *et al.*, Absorption and fluorescence studies of Sm ions in lead containing sodium fluoroborate glasses, *J. Lumin.* **131** (7), 1368 (2011). DOI: 10.1016/j.jlumin.2011.03.016.
25. M. Venkateswarlu *et al.*, Holmium doped Lead Tungsten Tellurite glasses for green luminescent applications, *J. Lumin.* **163**, 64 (2015). DOI: 10.1016/j.jlumin.2015.02.052.
26. K. S. Ojha, Structural and optical properties of PVA doped zinc sulphide thin films, *Optik* **127** (5), 2586 (2016). DOI: 10.1016/j.ijleo.2015.11.233.
27. R. P. Chahal *et al.*, UV irradiated PVA-Ag nanocomposites for optical applications, *Appl. Surf. Sci.* **343**, 160 (2015). DOI: 10.1016/j.apsusc.2015.03.074.
28. Basavarajeshwari M Baraker, and B. Lobo, Dispersion parameters of cadmium chloride doped PVA-PVP blend films, *J. Polym. Res.* **24**, 84 (2017).
29. E. Davis, and N. F. Mott, Conduction in non-crystalline systems V, *Philos. Mag.* **22** (179), 0903 (1970). DOI: 10.1080/14786437008221061.
30. K. Kiran Kumar *et al.*, Investigations on the effect of complexation of NaF salt with polymer blend (PEO/PVP) electrolytes on ionic conductivity and optical energy band gaps, *Physica B. Condens. Matter.* **406** (9), 1706 (2011)., DOI: 10.1016/j.physb.2011.02.010.
31. V. Raja, A. K. Sarma, and V. V. R. Narasimha Rao, Optical properties of pure and doped PMMA-CO-P4VPNO polymer films, *Mater. Lett.* **57** (30), 4678 (2003). DOI: 10.1016/S0167-577X(03)00384-7.
32. E. M. Abdelrazek, A. M. Abdelghany, and A. A. Aldhabi, Influence of manganese chloride filler on optical and structural properties of PVA/PVP films, *J. Mater. Sci.* **10** (1), 1 (2013).
33. T. A. Hamdalla, T. A. Hanafy, and A. E. Bekheet, Influence of erbium ions on the optical and structural properties of polyvinyl alcohol, *J. Spectrosc.* **2015**, 1 (2015). DOI: 10.1155/2015/204867.
34. R. R. Reddy, and Y. N. Ahammed, A study on the Moss relation, *Infrared Phys. Technol.* **36** (5), 825 (1995). DOI: 10.1016/1350-4495(95)00008-M.
35. C. Kittle, *Introduction to solid state physics*, Wiley and Sons, New York (1971), pp 321.
36. K. Sivaiah, and S. Buddhudu, Photoluminescence spectra of Sm^{3+} and Dy^{3+}:PVP polymer films, *Indian J. Phys.* **86** (12), 1079 (2012). DOI: 10.1007/s12648-012-0176-1.